

Dielectric Constant and Solvent Effect Investigation on *Listeria monocytogenes* InIB- β -sheet Conformation: an Ab initio-NMR study

E.Shirkhodae Tari¹ and M.Monajemi^{2,*}

¹ Ph.D. Student, Science and Research Branch, Islamic Azad University, Tehran, Iran

² Department of Chemistry, Science and Research Branch, Islamic Azad University, Tehran, Iran

ABSTRACT

InIB- the main external virulence factor of the bacterium *Listeria monocytogenes*- contains seven parallel β -strands at its concave face with a patches of five exposed aromatic amino acids as a hot spot for host receptor (Met) binding. For better understanding of energetic and physicochemical properties, (un)folding transition, binding affinity and magnetic shielding tensors of InIB-LRR- β -sheet ab initio computer-aided methods have been performed at the Hartree-Fock level. These calculations are based on the influence of solvent polarity as well as hydrogen bond donor and acceptor strength of it with respect to the self-consistent reaction field (SCRF) method using Onsager model. The optimized molecule with 6-31G(d,p) basis set in the gas phase was used as initial input for subsequent HF/SCRF calculations implementing 6-31G(d,p) atomic basis set to simulate the solvent effect. To gain further insight to solvent effects on aromatic amino acids ¹⁵N and ¹⁷O atoms engaged in hydrogen bonding with receptor, NMR studies have been carried out on the basis of gauge-including atomic orbital (GIAO) method at HF/6-31G (d,p) level of theory. HF calculations obtained with a good agreement by the presented experimental data and predict the most molecule instability in the solvents by low dielectric constants like THF and existence of a cooperativity among β -strands, physicochemically. There are various potential of hydrogen bond donors and acceptors among this unique, packed and exposed linearly arrangement of aromatic amino acids that have made it an ideal part for drug design.

Keywords: InternalinB, β -sheet (un)folding; Ab initio; Solvent effect, NMR calculations; Binding affinity

INTRODUCTION

Internalins from *Listeria monocytogenes* represent a distinct class of proteins that have been optimized for the specific interactions with different host cell receptors through the course of evolution. Invasiveness of this bacterium for mediating systemic infection is a trait that is acquired after the ability of attaching, internalizing and spreading in the several tissues and cell types of eukaryotic host cells expressing Met receptor such as epithelial, endothelial, hepatic cells and fibroblasts [1]. These characters are induced by Internalin B (InIB), a *Listeria* surface-associated virulence protein. InIB is structurally well characterized. It has a modular architecture comprised of an N-terminal cap domain, a LRR domain of 22

amino acid repeats and an inter-repeat region (IR) domain followed by a second repeat region that non-covalently anchors the protein to the bacterial cell wall [2,3].

The superfamily of leucine-rich repeat (LRR) proteins are a prominent group of proteins containing tandem repeats [4]. InIB LRR domain contains seven tandem β -strands that form a continuous β -sheet with neighboring strand in the concave side of the molecule.

A patches of five exposed aromatic amino acids (Phe104, Trp124, Phe126, Tyr170, Tyr214) stretching over the entire concave face of the β -sheet in close proximity, is considered as a

*Corresponding author: m_monajemi@yahoo.com

hot spot for host receptor binding [5]. Regarding the sample stability, folding and topology of repetitive proteins, they should more readily accessible in experiment and theory than other less regularly structured proteins of similar size [6]. The kinetics and thermodynamics of InIB and β -sheet folding have traditionally been studied by optical spectroscopies, calorimetry and scattering techniques [7,8]. Although these techniques provide crucial information about global structural transitions, but provide relatively little direct information about site-specific structural features particularly at the atomic levels.

With molecular models and statistical mechanics, it is promising to provide a microscopic view of the living system mechanisms. So we investigated the characteristic and (un)folding properties of InIB β -sheet and its aligned aromatic amino acids as the example to illustrate the microscopic analysis of macroscopic thermodynamics data that have performed up to now. On one hand, while the solvation free energy is more difficult to model, useful results can be obtained with simple approximations like *ab initio* Self-Consistent Reaction Field (SCRF) model. This method provides a powerful tool to investigate the extent of hydrogen-bonding and polarity/polarisability properties of the solvent and its influence on the physicochemical quantities [9]. On the other hand, *ab initio* multi-nuclear NMR calculations is taking an important position in understanding the functions of biomolecules and the role of their structure in drug design [10]. Atoms in different environments experience different amount of shieldings. So, the lack of experimental NMR data motivated us to calculate NMR shielding tensors of nitrogen and oxygen atoms of aromatic β -sheet residues and in a wide range of solvents encompassing a broad spectrum of polarity and hydrogen-bonding properties in the basis of gauge-including atomic orbital (GIAO) method [11]. These findings help to deeper understanding of InIB β -sheet stability and (un)folding pathways and comparing chemical shifts variations under some conditions such as different dielectric constant values. Changes in solvent polarity may influence intermolecular shielding of InIB β -sheet. Thereby, these computer simulations complement the macroscopic views of the experimental processes and open up practical strategies to discover novel therapeutics and protein-based drug design to combat this insidious bacterium.

THEORETICAL METHODS

The coordinates of the amino acids distributed in seven tandem β -strands (residues 4-6 in each repeat) in InIB β -sheet was taken from the X-ray coordinate file (Protein Data Bank (PDB) entry code: 1D0B) [7]. Hydrogen atoms not included in the PDB file were generated by the standard MM procedures in HYPERCHEM package [12]. The concave face of β -sheet and linear arrangement of aromatic rings is shown in (Fig.1) and the atom numbering of five aromatic amino acids used throughout the text is included.

We constructed three fragments of β -sheets that is introduced by part1 (2 first β -strands), part2 (2 second β -strands) and part3 (three third β -strands) (Fig. 1). After preparing appropriate models, all fragments were optimized with STO-3G, 3-21G and 6-31G (d,p) basis sets in the gas phase at the Hartree-Fock (HF) level of theory to determine the molecular geometry with the GAUSSIAN 98 suite of programs [13].

The HF optimized parameters were used as initial input for subsequent HF/SCRF calculations at HF/6-31G (d,p) level of theory in five different solvents including water, DMSO, ethanol, acetone and tetrahydrofuran (THF). The simplest SCRF model is based on the Onsager's reaction field theory of electrostatic solvation. In this model the solvent is considered as a uniform dielectric with a given dielectric constant (ϵ). The solute is assumed to occupy a spherical cavity of radius a_1 inside the solvent. The permanent dipole moment of the solute will induce a multipole in the surrounding medium, which will interact with the permanent molecular dipole, culminating to net stabilization [14]. The cavity radii for the SCRF calculations were determined from the estimated molecular volume of the three parts. Consequently, for estimating solvent effects on the nitrogen and oxygen atoms of aromatic LRR residues shieldings and magnetic susceptibilities, HF/NMR calculations based on GIAO method with 6-31G(d,p) basis set, were performed [15].

RESULTS AND DISCUSSION

β -Sheet Conformation in Different Media

Table 1, provides results for total energies and dipole moments of β -sheet parts in gaseous phase and solvent media. As it appeared the dipole moment

values are increased on going from the solvent of high ϵ to lower ϵ . Also, the total energies have been obtained more negative. It means that the physical properties of three β -sheet parts in low-polar solvents on essentially similar scaffold are disrupted and there is direct correlation between dipole moment and the order of instability under SCRF conditions. β -sheets needs to charge distribution alongside the whole molecule for conserving of their folding and activity, so increasing trend of dipole moment is indicative of focused electron clouds and somehow denaturation [15].

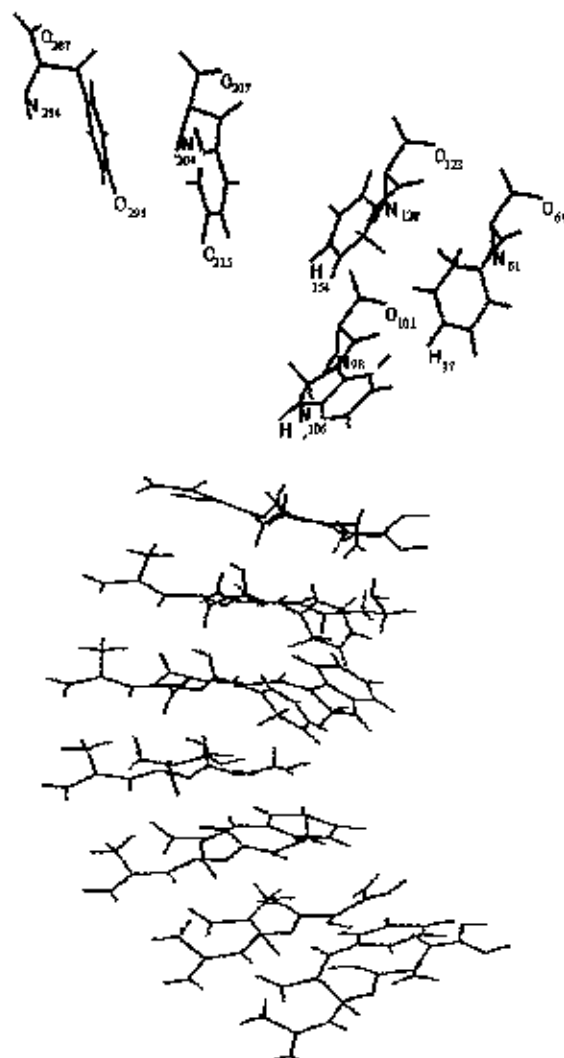


Fig. 1. The concave face of β -sheet including five exposed aromatic amino acids and atom numbering were used for the analysis

On the other hand, the solvation energy calculated by the SCRF method corresponds to the electrostatic contribution to the free energy of

solvation. This method evaluates only the electrostatic component of solvation [16]. T.Lazaridis and M.Karplus reported that the electrostatic solvation energies in unfolded state are more negative primarily because back-bone hydrophobic hydrogen bonding groups buried in the native state become more exposed to the solvent [17]. Most of the β -sheets fold with an identifiable core of hydrophobic residues which in the case of InIB β -sheet it is more significant and this buried hydrophobic group become accessible in low-polar solvents culminating to protein unfolding [17]. So the negative trend seen in total energies from water to THF is representative of unfolding of the molecule, too. The molecule has the most stabilities in water and the shifts obtained in dipole moment for polar solvents are relatively closed to each other and gradually towards the low-polar solvents the deviations will be more pronounced in which in THF there is the least stabilities. As it appeared all of the conclusions are in a good agreement with each other. It is worth noting that all three parts in performed calculations react in a similar fashion. So, it seems that there is a cooperativity among the β -strands in which taken together determine the whole β -sheet character.

Multi-nuclear NMR Studies in Vacuum and Solvent Media

It is valuable to calculate quantum mechanical properties of nuclei in the basis of NMR assignments in order to probe ligand-receptor binding via determining of chemical shift mapping and dynamics. Different solvents and changes in solvent polarity may influence intermolecular shielding of InIB β -sheet. Typically three principal eigenvalues (σ_{11} , σ_{22} , σ_{33}) and the isotropic value (σ_{iso}), the anisotropy of the tensor (σ_{anis}) can be predicted by suitable quantum mechanical computations [18]. It is useful to express shielding tensor data using three other parameters as well as the principal components including $\Delta\sigma$ (shielding anisotropy tensor), δ (chemical shift) and η (shielding asymmetry) [18].

As it appeared from Table 2, there is only a small dependence of the nuclear shieldings on the various environments and the solvents employed is likely to enter into rather weak molecular interactions with the solutes in which a small

change in chemical shift values is seen while going from gaseous to liquid phase environment. This apparent insensitivity of ^{15}N and ^{17}O atoms shieldings to solvent effects seems to stem from the rigidity of this molecule. As a result, this repetitive unite can easily accommodate a large range of repeats in which there are between six LRRs in InIC to 15 LRRs in InIA [19]. Also, these theoretical values of the nuclear shieldings can be compared with the experimental data, because of a small solute-to-solvent interactions. Nevertheless, gas to solution shifts of the N120 in Phe126 amino group and O101 in Trp124 carboxyl group shieldings are relatively more pronounced.

On the other side, according to the Table 2, there are some differences between the aromatic rings and backbone carboxyl and amino groups nitrogen and oxygen atoms chemical shifts in solvent media. It can be hypothesized that the solvent effect is the major differences between the core and more exposed atoms. Also, on one hand, well-known ring current effects on N and O atoms attached to the aromatic rings can influence these atoms chemical shift variations and on the other hand, intramolecular H-bonds between internal atoms forming this secondary structure (β -sheet) impede the formation of intermolecular H-bonds to solvent. So, it seems that the saturated interfaces between β -strands by hydrogen bonds, can influence the physicochemical behavior of the molecule.

According to the (Fig. 2a) the hydrogen bonding of THF with NH of the Trp indole ring has more effect on the ^{15}N chemical shifts consequently significant effect on the electronic

configuration of indole and then amino acid. As discussed above, the most instability represents in the THF. Furthermore, the downfield movement in chemical shift seems to arise from increasing delocalization of the nitrogen lone pair by the n -electron system which results in increased anisotropic deshielding with the decreasing polarity of the medium and the most density changes is resulted from the interaction with THF. The extension of π resonance system in indole ring can play a considerable role in this behavior, too. The only exception is DMSO that induces the least chemical shift in Trp-indole-N atom.

In Tyr-phenol-O atoms, this trend is identical and inverted and the delocalization of electron lone pairs and shielding variations follow the polarity of the solvent in the sense of enhanced deshielding with the increasing polarity (Fig. 2a). This character likely is more stressed by forming partial double bond of the C-O bond on aromatic ring inducing by π -resonance system. It is to be noted that regarding to the Tyr170-O ring, Tyr214-O ring has the maximum chemical shift values in all the environments (Table 2).

The anisotropic values of amino groups nitrogen atoms predict the order of deshielding as $\text{N204} > \text{N284} > \text{N120} > \text{N98}$ in different media. So, Tyr-170-N and Trp-124-N amino groups have the most and the least chemical shift values in above-mentioned environment, respectively (Fig.2b). The same deshielding trend is seen for carboxyl groups oxygen atoms in which Tyr-170-O and Trp-124-O carboxyl groups undergo the most and least chemical shifts in different media (Fig. 2b).

Table 1. Calculated total energies E (in kcal/mol), dipole moments μ (in Debye) of β -sheet parts versus dielectric constant ϵ at the HF/6-31G(d,P) level of theory

		E(kcal/mol)					
		μ (Debye)					
ϵ	Vacuum	Water	DMSO	Ethanol	Acetone	THF	
	1	78.39	46.8	24.55	20.7	7.58	
Part 1	-1520373.916 8.672	-1520373.917 0.670	-1520373.921 8.676	-1520373.951 8.724	-1520373.973 8.739	-1520375.157 10.657	
Part 2	-1531379.36 4.3	-1531379.361 4.3045	-1531379.362 4.3049	-1531379.369 4.3364	-1531379.375 4.3591	-1531379.685 5.601	
Part 3	-2298427.436 8.659	-2298426.872 8.96	-2298426.876 8.97	-2298426.908 9.06	-2298426.933 9.13	-2298429.461 13.08	

Table 2. NMR shielding values of ^{15}N and ^{17}O (in ppm) calculated for aromatic amino acids at HF/6-31G level of theory in vacuum and solvent media

Gas Phase											
Atom	Phe126			Trp124			Tyr170			Tyr214	
	N120	O123	N106	O101	N90	O215	N204	O207	O295	N284	O207
σ_{iso}	-119.104	-408.0687	222.1179	-380.4835	-115.848	-284.509	-146.3503	-425.3974	-339.5922	-144.6704	-391.828
σ_{anis}	568.9443	1222.095	98.9124	1179.4384	565.6336	1001.5224	600.4745	1255.7634	1099.4062	593.8487	1200.189
$\Delta\sigma$	-606.592	1222.095	98.91235	1179.4384	-602.138	1801.52235	-680.7795	1255.7634	1099.4062	-670.8180	1200.189
η	0.87587	0.63376	0.123076	0.617318	0.87875	0.674712	0.764079	0.63176	0.722086	0.77054	0.621135
δ	-404.3945	814.73	65.9416	786.257	-401.426	667.4416	-453.853	837.1756	732.9375	-447.2068	800.126
ϵ	water										
σ_{iso}	-118.097	-407.6058	222.1715	-379.9448	-115.900	-284.5595	-146.3498	-425.4185	-339.5758	-144.6139	-391.8638
σ_{anis}	567.802	1221.1996	98.9749	1178.7672	565.8846	1801.4416	600.4589	1255.7949	1099.3819	593.8107	1280.2698
$\Delta\sigma$	-604.545	1221.1995	98.97945	1178.76715	-602.091	1441.4416	-688.785	1255.7949	1099.3819	-670.7473	1200.2698
η	0.87844	0.63333	0.12318	0.617522	0.87973	0.674746	0.764619	0.631787	0.722077	0.770594	0.621103
δ	-403.030	814.133	65.9863	785.8448	-481.393	667.761	-453.857	837.1966	732.9216	-447.1649	880.1799
ϵ	DMSO										
σ_{iso}	-118.3877	-407.778	222.1349	-380.1348	-115.960	-284.5577	-146.3513	-425.4298	-339.5759	-144.6134	-391.8696
σ_{anis}	568.2067	1221.49	98.9084	1179.6165	565.8718	1001.636	600.4589	1255.8092	1099.3023	593.8089	1280.2815
$\Delta\sigma$	-605.188	1221.490	98.9084	1179.6165	-602.257	1801.6361	-680.7954	1255.8093	1099.3823	-670.752	1280.2816
η	0.87778	0.63354	0.122316	0.61744	0.87917	0.6747353	0.76399	0.6317936	0.722069	0.770577	0.621117
δ	-403.459	814.3266	65.939	786.011	-401.505	647.7574	-453.8636	837.2062	732.9215	-447.168	880.1877
ϵ	Ethanol										
σ_{iso}	-118.156	-407.6187	222.2632	-379.9643	-115.934	-283.4939	-146.3548	-425.5142	-339.3805	-144.6059	-391.9049
σ_{anis}	567.8874	1221.236	99.1346	1178.7883	565.9116	999.0226	600.4286	1255.9279	1098.631	593.7865	1200.3324
$\Delta\sigma$	-644.670	1221.236	99.1341	1178.7883	-602.158	999.0226	-680.8252	1255.9279	1098.42105	-670.7384	1200.3324
η	0.878338	0.633337	0.120425	0.6175	0.879612	0.671773	0.763826	0.631872	0.719928	0.770546	0.621156
δ	-403.114	814.1574	66.3452	785.8589	-401.439	666.0151	-453.8834	837.2853	732.4141	-447.1589	800.2223
ϵ	THF										
σ_{iso}	-119.8449	-487.5723	222.6821	-380.2773	-116.596	-282.1324	-146.3702	-427.9761	-339.1012	-144.4749	-393.3879
σ_{anis}	570.7951	1221.7141	99.8112	1179.0267	566.7948	997.5631	599.6511	1259.1867	1097.712	593.6569	1203.0302
$\Delta\sigma$	-608.024	1221.71415	99.8112	1179.0267	-603.418	997.5631	-681.990	1259.1867	1097.7321	-671.297	1203.0302
η	0.87754	0.632606	0.11957	0.61661	0.878316	0.669683	0.758535	0.6317908	0.70222	0.766897	0.622417
δ	-405.35	814.4862	66.7661	786.6178	-402.279	665.234	-454.660	839.4578	731.5431	-447.5317	802.0201

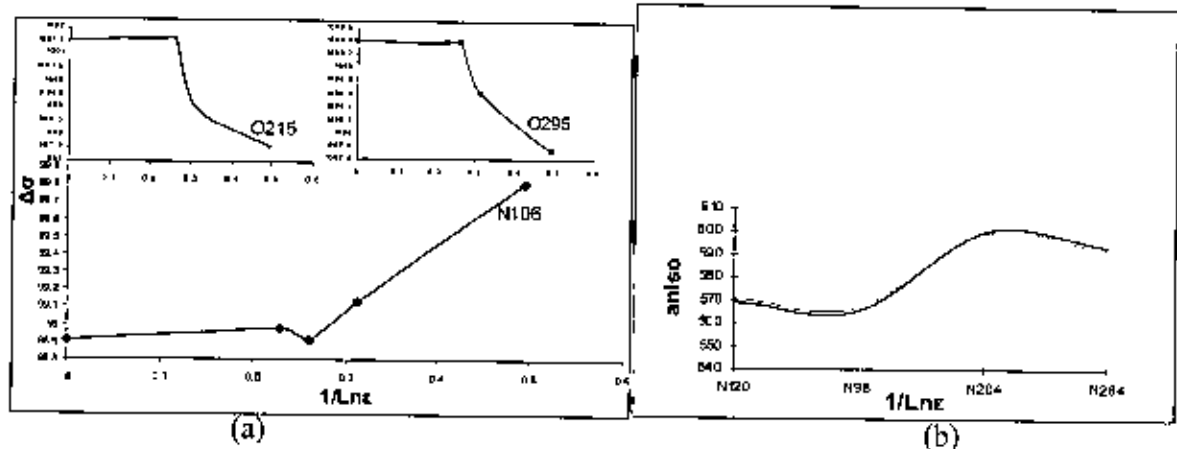


Fig. 2. The graphs of a) shielding anisotropy tensors of Trp-indole- ^{15}N and two Tyr-phenol- ^{17}O atoms, b) anisotropy shieldings of amino groups- ^{15}N and shielding anisotropy tensors of carboxyl groups- ^{17}O in aromatic amino acids (in ppm) for different values of the dielectric constant $[1/\epsilon]$ at the 6-31G level of theory in the basis of GIAO method.

So we can hypothesize, Y170 which is centrally located at this exposed formed string on the concave face of the InIB, likely play an important role in receptor binding. In spite of F104, F126, Y170 and Y214 which occupies third residues of the β -strands of repeats 2,3,5 and 7 of the LRR domain respectively, W124 is located at position 1 of the third repeat. So it is arranged alongside the central aromatic string and is at a lesser extent involved in solvent interactions [9]. Because the solvent effect is the major difference between the internal and surface residues [20].

CONCLUSION

One area where ab initio calculations can be useful, is the process of protein (un)folding and binding between a macromolecule and a ligand. Since high-affinity binding events between InIB LRR and Met is necessary for internalization of bacterium *Listeria monocytogenes* into the host cells, it is desired to understand the energetic and structural details of such interactions via calculations carried out in the gas phase incorporating with

environmental effect via solvent continuum. As more detailed data become available especially about the strength and specificity of noncovalent intra and inter molecules interactions at the atomic level, these events can be controlled more towards desirable directions particularly in drug design field.

Ab initio HF calculations obtained with a good agreement by the presented experimental data and predict a relatively significant independence of the isolated InIB β -sheet geometry on the environmental effects especially in polar solvents. This is clearly an advantage for a more closely packing molecule exposed to the hostile proteolytic host environment. However, this molecule varies mostly in the solvents by low dielectric constants like THF and there is a cooperativity among β -strands, physicochemically. On the other hand, the aromatic rings atoms especially Trp-indole-N and Tyrs-phenol-O atoms play a key role in receptor binding and controlling β -sheet folding and their behavior in used solvents are reversed.

REFERENCES

- [1] S.S.Chatterjee, S.Otten, T. Hain, A.Lingnau, J. Wehland, E. Domann and T. Chakraborty. *International Journal of Medical Microbiology*. 296(2006)277-286.
- [2] W.Schubert, G.Gibel, M.Deipholz, A.Darji, D.Klore, T.Hain, T.Chakraborty, J. Wehland, E.Domann and D.W.Heinz, *J.Mol.Biol.* 312(2001) 783-794.
- [3] M.Marino, M.Banerjee, R.Jonquieres, P.Cossart and P.Gbosh, *MBO J.* 21(2002) 5623-5634.
- [4] B.Kobe and A.V.Kajava, *Curr. Opin. Struct. Biol.* 11(2001)725-732.
- [5] M.P.Machner, S.Frese, W.Schubert, V.OrianRousseau, E.Gheradi, J.Weiland, H.H.Niemann and D.W.Heinz. *Molecular Microbiology*. 48(6) (2003)1525-1536.
- [6] W.Schubert, G.Gobe and M.Diepholz, *J. Mol. Biol.* 312(2001)783-794.
- [7] N.Courtemanche and D.Barrick, *Protein Science*. 17(2008)43-53.
- [8] A.Freiberg, M.P.Machner, W.Pfeil, W.Schubert, D.W.Heinz and R.Seckler, *J. Mol.Biol.* 337(2004)453-461.
- [9] V.Sathyabama, K.Anandan and R.Kanagaraju. *Journal of Molecular Structure (Theochem)*. 897(2009)106-110.
- [10] C.Zaccari, A.Anderson, *Chemistry & Biology* 10(9) (2003)787-797.
- [11] B.R.Donald and J.Martin, *Progress in Nuclear Magnetic Resonance Spectroscopy*. 55(2009)101-127.
- [12] M.Mooajjemi, L.Mahdavian and F.Mollaamin, *Bull. Chem. Soc, Ethiop.* 22(2008) 277-286.
- [13] S.Huzinaga, M.Andzelm, M.Klobukowski, E.Radziu-andzelm, Y.Sakai and H. Tatewaki, Elsevier, amsterdam.
- [14] M.Monajjemi, B.Honarparvar, H.Haeri and M.Heshmat, *Russ.J.Phys.* 80(2006)40-44.
- [15] E.RG Main, A.Lowe, S.Moehrie, S.Jackson and L.Regan, *Current Opinion in Structural Biology*. 15(2005)464-471.
- [16] G.Nardini and D.N.Sathyanarayana, *Journal of Molecular Structure (Theochem)*. 590(2002)171-181.
- [17] Th.Lazaridis and M.Karplus. *Biophysical Chemistry*. 100(2003)367-395.
- [18] R.Harris, E.Becker, S.Menczes, P.Granger, R.Hoffman and K.Zilm, *Solid State Nuclear Magnetic Resonance*. 33(2008)41-56.
- [19] Y.Tsai, R.Orsi, K.Nightingale and M. Wiedmann, *Infection, Genetics and Evolution*. 6(2006) 378-389.
- [20] Qi.Gao, S.Yokojima, T.Kohno, T.Ishida, D.G.Fedorov, K.Kitaura, M.Fujihira and Sh. Nakamura, *Chemical Physics Letters*. 445(2007) 331-339.